Supramolecular assemblies of photochromic benzodithia-18-crown-6 ethers in crystals, solutions, and monolayers†

Olga A. Fedorova,*[a] Yuri V. Fedorov,[a] Artem I. Vedernikov,[a] Olga V. Yescheulova,[a] Sergei P. Gromov,[a] Michael V. Alfimov,[a] Lyudmila G. Kuz'mina,[b] Andrei V. Churakov,[b] Judith A. K. Howard,[c] Sergei Yu. Zaitsev,[d] Tatyana I. Sergeeva[d] and Deitmar Möbius[e]

[a] *Photochemistry Center, Russian Academy of Sciences, 7A Novatorov str., Moscow, 117421, Russia. E-mail: fedorova@photonics.ru*
[b] *Institute of General and Inorganic Chemistry, Russian Academy of Sciences, 31 Leninskii pr., Moscow, 117909, Russia*
[c] *Chemistry Department, University of Durham, South Road, Durham, UK DH1 3LE*
[d] *Institute of Bioorganic Chemistry, Russian Academy of Sciences, 16/10 Miklukho-Maklaya str., Moscow, 117871, Russia*
[e] *Max-Planck-Institute of Biophysical Chemistry, Postfach 2841, D-37018 Göttingen, Germany*

Received (in London, UK) 19th November 2001, Accepted 21st January 2002
First published as an Advance Article on the web 10th April 2002

We studied the assembly of dithiacrown ether styryl dye (CSD) molecules in crystals, solutions, and films in the presence of metal cations. X-Ray diffraction data allowed us to conclude that the anion affects the supramolecular architecture of CSDs in the crystal, specifically, the type of stacking of the dye molecules. In solution, in the presence of Pb^{2+}, CSD molecules with the betaine structure spontaneously form dimeric complexes consisting of two dye molecules and two metal cations, with a fixed mutual arrangement of the double bonds. The dimer complex is stable due to coordination between the anion substituent of one molecule and the metal cation located in the crown ether cavity of the other molecule. Irradiation of the dimer complexes leads to regio- and stereoselective [2 + 2]-cycloaddition, giving only one cyclobutane derivative of the eleven theoretically possible products. The other photoreaction studied for CSDs is reversible *Z–E* isomerization. Due to its specific structure, the betaine-type CSD is able to form the 'anion-capped' *Z*-isomer. Intramolecular coordination in the 'anion-capped' isomer enhances its stability and causes a sharp deceleration of its dark *Z–E* isomerization. The amphiphilic CSD forms relatively stable monolayers on distilled water and various aqueous salt subphases. The results obtained indicate that it is possible to distinguish between two types of the dye monolayer structures based on the presence of alkali or heavy metal cations in the aqueous subphase.

Introduction

The assembly of molecular compounds into large and functional arrays can be achieved by employing various types of interaction. These include weak directional intermolecular interactions, such as hydrogen bonds, donor–acceptor and stacking interactions, or stronger coordination and covalent bonds.[1] One approach to the modelling of supramolecular assemblies involves the synthesis of covalently bonded donor–acceptor dyads, triads, and pentades.[2] A great number of luminescent polynuclear transition metal complexes have been synthesized and their ability to absorb visible light with subsequent luminescence and to be subjected to reversible multielectron redox processes has been studied.[3] In the crystal engeneering, the greatest interest is focussed on the investigation of directional weak interactions resulting in three-dimensional arrays and networks based on linear ligands bound to metal ions.[4] The attachment of the ligand centre to a polymer body or a supramolecular assembly of ligands in monolayers and LB films provides a means for the design of systems capable of displaying selection and photoswitching properties.[5] These systems are interesting in the context of fundamental science and promising for a variety of applications, such as components in molecular electronics, photoswitchable molecular devices, and luminescence sensors for metal cations.[6] Appropriate molecular design of supramolecular structures formed upon self-assembly in solutions, monolayers, or crystals containing photosensitive units makes it possible to create a series of simple photoswitchable molecular devices.[7]

Previously,[8] we have reported that integration of a styryl dye fragment with a benzocrown ether results in novel photochromic compounds, namely, crown-containing styryl dyes (CSDs), which are able to bind alkaline earth metal cations and exhibit interesting physico-chemical properties. For instance, photochromic CSDs make it possible to control the binding of alkaline earth metal cations by virtue of light because they are capable of 'taking off' and 'putting on' their anionic 'cap' on exposure to light of different wavelengths. Such compounds are promising for the development of reagents for optical determination of metal cations and as components of photoswitching molecular devices.

Development of an improved method for the synthesis of formyl derivatives of benzothiacrown ethers resulted in the synthesis of novel styryl dyes[9] incorporating a benzodithiacrown ether moiety. The thiacrown compounds exhibit a clear-cut preference for complex formation with heavy metal ions. It was shown that in combination with an appropriate chromophore, this selectivity can be enhanced or modulated

† Electronic supplementary information (ESI) available: crystal data, data collection, and structure solution and refinement parameters. See http://www.rsc.org/suppdata/nj/b1/b110630a/

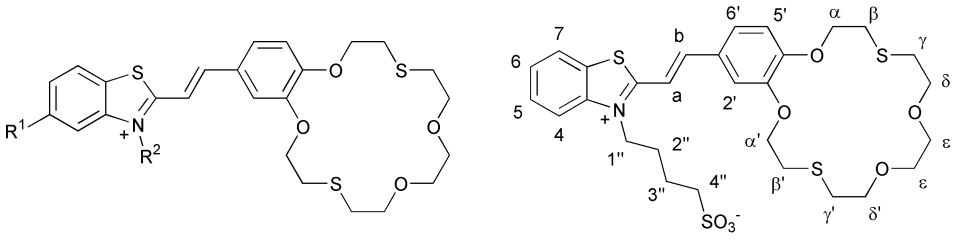

1a: $R_1 = H$, $R_2 = Me$ (I^-)
1b: $R_1 = H$, $R_2 = Me$ (ClO_4^-)
2 : $R_1 = H$, $R_2 = (CH_2)_4SO_3^-$
3: $R_1 = NHCO(CH_2)_{16}Me$, $R_2 = (CH_2)_4SO_3^-$

Scheme 1

by absorption of light. Specifically, the benzodithia-18-crown-6 styryl dye **2** becomes 11 times more selective towards Hg^{2+} upon *E–Z* photoisomerization.

We concentrated attention on CSDs involving a benzodithia-18-crown-6 ether moiety and proposed that these compounds can be self-assembled in the crystals, solutions, and films in the presence of metal cations. The mode of CSD assembly in the solid state, in solution, and in films influences the complexing and photochromic properties of the CSDs. In this work, we studied CSDs **1a**, **1b**, **2**, and **3** (Scheme 1); the synthesis of the dyes has been published previously.[9]

Results and discussion

X-Ray diffraction study

The molecular and crystal structures of iodide (**1a**) and perchlorate (**1b**) salts of benzodithiacrown ether styryl dye were determined using single crystal X-ray diffraction analysis. Fig. 1 and 2 show the general view and atom numbering schemes for all structural units in **1a** and **1b**. The most important geometrical parameters of the crown ether dye cation in **1a** and **1b** are given in Table 1.

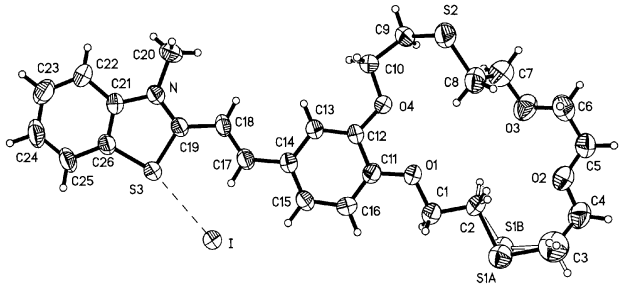

Fig. 1 Structure of **1a** with 50% probability thermal anisotropic parameters.

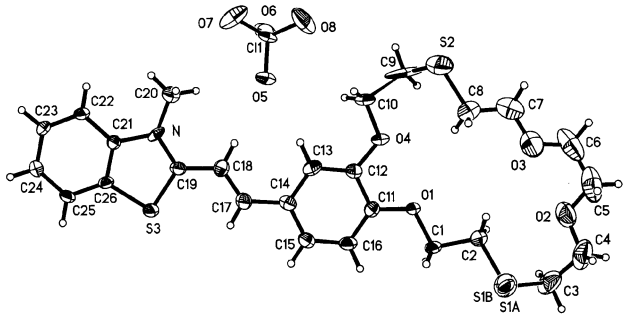

Fig. 2 Structure of **1b** with 50% probability thermal anisotropic parameters.

The dye molecules in both structures are nearly planar; the twisting of the planar fragments about the corresponding formally single bonds [C(14)–C(17) and C(18)–C(19)] does not exceed 6° and the two rings of the benzothiazolium system are almost coplanar (Table 1). This geometry is favourable for conjugation over the whole cation, except for the crown ether subunit.

The corresponding bond lengths in the molecular cations of **1a** and **1b** are similar within the limits of experimental error. The C(11)–(16) benzene ring shows nearly complete bond delocalization. The C(17)–C(18) ethylene bond is essentially localized. The lengths of this bond [1.338(7) and 1.322(8) Å for **1a** and **1b**, respectively] are significantly smaller than the lengths of the C(17)–C(14) [1.439(6), **1a**, and 1.473(8) Å, **1b**] and C(18)–C(19) [1.449(6), **1a**, and 1.442(8) Å, **1b**] formally single bonds and than the average bond length in the C(11)–(16) benzene ring (1.39 Å) with the delocalized bond system.

The O(1) and O(4) atoms are in conjugation with the aromatic ring. The corresponding C–C–O–C torsion angles are close to 0°; the bond angles at these particular O atoms (*ca.* 117–119°) are greater than those at the two other atoms (111–113°), suggesting that the O(1) and O(4) atoms are in the sp^2 hybridization state, whereas O(2) and O(3) are sp^3 hybridized.

The most significant geometric differences between the molecular cations of **1a** and **1b** are in the crown ether fragments. Fig. 3 shows the benzocrown ether fragments of **1a** and **1b** superimposed onto the benzene rings, which clearly displays the similarities and differences in the crown ether geometry. In the quadrangle of O atoms, two O···O distances are short (*ca.* 2.5 and 2.8 Å) and the other two O···O distances are long (*ca.* 4.8 and 5.0 Å) for both dye cations. In both structures, the sulfur atoms are located outside the macrocycle. Structures **1a** and **1b** are disordered in the vicinity of the S(1) atom. In **1b**, the S(2) atom and the nearest carbon atoms are also disordered over several positions. This disorder reflects the high flexibility of the crown ether macrocycle, at least in the regions of the sulfur atoms, and indicates the occurrence of loosely packed areas in the crystal. This may be one of the reasons for the poor crystallization of these compounds.

Comparative analysis of the crystal packing in **1a** and **1b** is of special interest. The presence of different anions resulted in different packing of the crown ether dye cations (Fig. 4 and 5). In the crystal of **1a**, the dye molecules form parallel, centrosymmetrically related 'head-to-tail' pairs due to stacking interactions (Scheme 2).

Actually, no traditional infinite stacks of dye cations are observed in the crystal. The two nearest pairs (**b** and **c**) related to a selected pair (**a**) through another system of symmetry centres are markedly shifted in the parallel planes (Scheme 3).

Any of the two adjacent pairs (**a** and **b** or **a** and **c**) contact through the peripheral benzene rings of the benzothiazolium subunits. The shortest contact is C(24**a**)···C(26**b**) (3.64 Å), the C(25**a**)···C(26**b**) and C(21**a**)···C(25**b**) contacts being longer (3.74 Å).

Table 1 Selected geometrical parameters for the crown ether dye cation in **1a** and **1b**

	1a	1b		1a	1b
Bond lengths/Å			**Dihedral angles/°**		
C(11)–C(12)	1.408(6)	1.396(8)	$P(1)/P(2)^a$	2.8	4.4
C(12)–C(13)	1.388(6)	1.395(8)	$P(2)/P(3)^a$	1.6	6.4
C(13)–C(14)	1.411(6)	1.410(9)	$P(3)/P(4)^a$	1.4	0.5
C(14)–C(15)	1.384(7)	1.384(9)			
C(15)–C(16)	1.388(7)	1.389(9)	**Torsion angles/°**		
C(16)–C(11)	1.380(6)	1.381(8)	C(16)C(11)O(1)C(1)	1.4	−3.5
C(14)–C(17)	1.439(6)	1.473(8)	C(13)C(12)O(4)C(10)	3.1	1.1
C(17)–C(18)	1.338(7)	1.322(8)			
C(18)–C(19)	1.449(6)	1.442(8)	**Distances/Å**		
C(19)–N	1.318(6)	1.349(7)	O(1)···O(2)	4.912	5.047
C(19)–S(3)	1.716(4)	1.715(6)	O(1)···O(4)	2.549	2.539
S(3)–C(26)	1.728(5)	1.753(6)	O(2)···O(3)	2.778	2.776
N–C(21)	1.392(5)	1.443(7)	O(3)···O(4)	4.820	4.969
C(21)–C(26)	1.395(7)	1.380(8)			

[a] $P(1)$, $P(2)$, $P(3)$, and $P(4)$ are the planes through the C(11)–(16), C(14)–(19), C(19)S(3)C(26)C(21)N, and C(21)–(26) atomic groups, respectively.

The two antiparallel ethylene groups in the pair are in close vicinity to each other. The C(17)···C(18′) and C(18)···C(17′) distances are both 3.63 Å. This rather short distance, together with the parallel arrangement of the ethylene fragments, is favourable for [2 + 2] cycloaddition, which should lead to one of the eleven cyclobutane isomers, presented in Scheme 4.

However, such photochemical reactions have been observed previously only for crown ether styryl dye complexes with

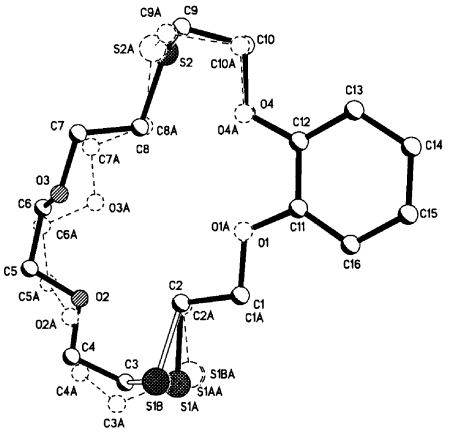

Fig. 3 Superposition of benzocrown ether subunits of **1a** and **1b**.

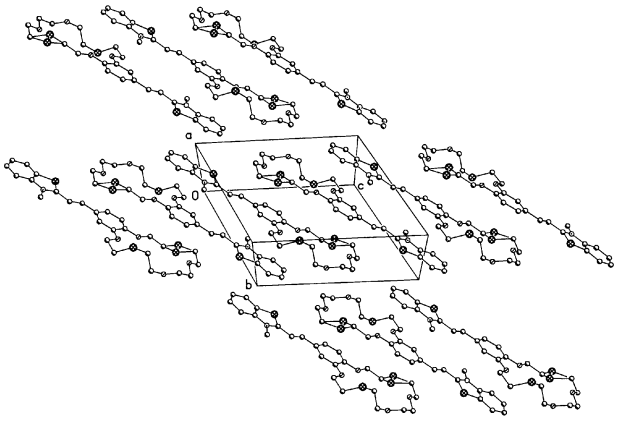

Fig. 4 Crystal packing of the molecular cations in **1a**.

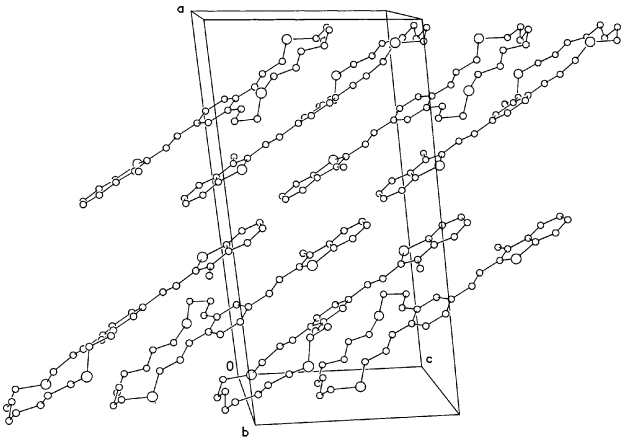

Fig. 5 Crystal packing of the molecular cations in **1b**.

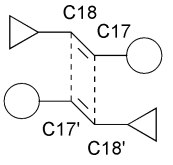

Scheme 2

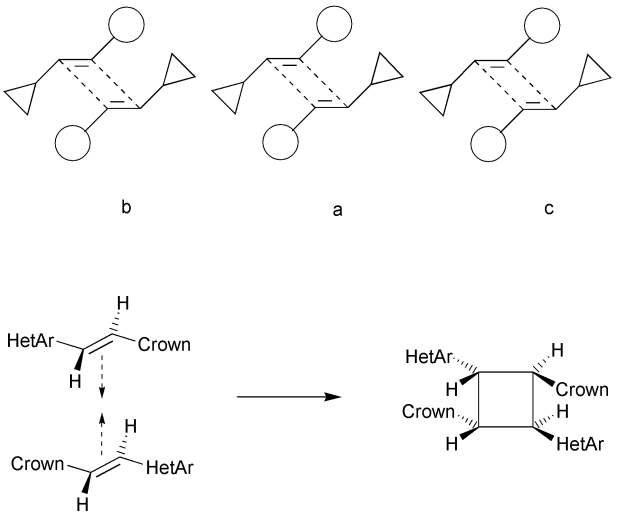

Scheme 4

metal cations (Mg^{2+} and Ca^{2+}) incorporating a rather long side chain, $(CH_2)_nSO_3^-$, at the heterocyclic nitrogen atom.[1d] Theoretical calculations (molecular mechanics, force field MMP2, and MMX methods) provided an interpretation of the regio- and stereoselectivity of these reactions.[10] These properties are due to the formation of fairly rigid dimeric structures with parallel and closely arranged ethylene groups due to coordination of each of the two metal cations to the crown ether oxygens of one molecule and the SO_3^- group oxygens of the other molecule.

In the structure of **1a**, two molecules form an antiparallel pair due to the stacking interaction. This interaction is not strong enough to fix the dimeric structure in a dilute solution, although this might be expected in concentrated solution.

Conversely, in the crystal of **1b**, the dye cations form infinite stacks (Fig. 5). The cations are arranged according to the 'head-to-head' pattern. Any two adjacent cations in a stack are related by the crystallographic glide plane *c*. In a stack, the near planar fragments of adjacent molecules are strongly shifted with respect to each other in parallel planes. Moreover, any two adjacent molecules in a stack have a crossed mutual arrangement of the ethylene fragments, unfavourable for [2 + 2] cycloaddition (Scheme 5).

In both crystals, the crown ether fragments form loosely packed channels with long intermolecular distances, most of them being longer than the sums of the van der Waals radii. In **1a**, these channels surround the closely arranged ethylene fragments in the pairs. In view of this specific 'soft' environment, we intend to study in the future whether the above-mentioned [2 + 2] photocycloaddition can be attained on irradiation in the solid state, at least in several regions of the single crystal.

In our opinion, one of the most important reasons for the difference in the crown ether cation packing in **1a** and **1b** is the influence of the anions. In the crystals of **1b**, ClO_4^- does not participate in the weak specific interactions with other atoms; the anions occupy cavities in the packing of the dye molecules in the vicinity of the crown ether subunits. Conversely, the I^- anions in **1a** participate in weak interactions with the molecular cations. Fig. 6 shows the system of weak interactions of the I^- anion. The corresponding contacts [I···H(20A)^i 3.00, I···C(20)^i 3.875, I···H(20G)^j 2.94, I···C(20)^j 3.874, I···H(10A)^i 3.03, I···C(10)^i 3.79, I···S(3)^k 3.97 Å, where the symmetry transformations are as follows: i = *x*, *y*, *z*; j = 1 − *x*, 1 − *y*, 1 − *z*; k = −*x*, 1 − *y*, 1 − *z*] are rather short, less than the sums of the corresponding van der Waals radii: I and H 3.4, I and C 4.0, I and S 4.2 Å. It can be seen that the I^- anion links the cations of two neighbouring levels of one stack and also two adjacent stacks. Hence, we can conclude that the

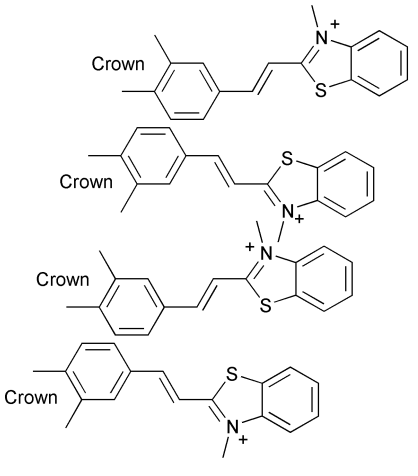

Scheme 5

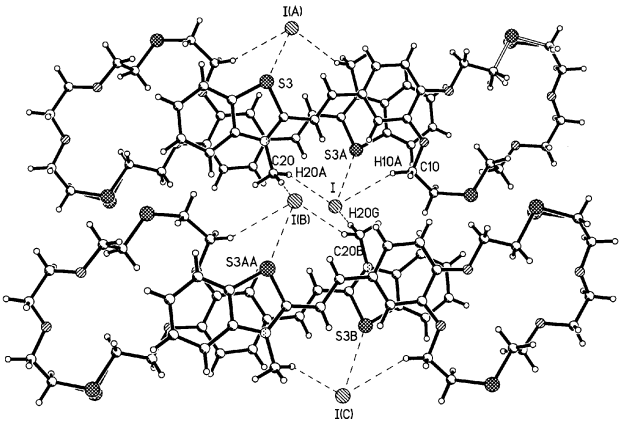

Fig. 6 Mutual arrangement of the molecular cations and the I^- anions in the crystal of **1a**.

I^- anion affects the supramolecular architecture of **1a**, specifically, the type of dye molecule stacking.

Complex formation with Pb^{2+} and photochemistry of dyes 1b and 2 in solution

As expected, the electronic absorption spectra of CSDs (*E*)-**1b** and (*E*)-**2** in MeCN are nearly identical because these dyes contain the same chromophoric components (Fig. 7). Of the cationic dyes (*E*)-**1a** and **1b**, the dye **1b** was choosen for study as it contains the same anion as $Pb(ClO_4)_2$, used in the complex formation experiments. This salt is well dissolved and fully dissociated in MeCN.

The long wavelength band in the absorption spectra (LAB) of (*E*)-**1b** and (*E*)-**2** undergoes hypsochromic shifts equal to 22 and 20 nm, respectively, on the addition of lead perchlorate to solutions of **1b** or **2** in MeCN, due to complex formation (Scheme 6, Fig. 7 and 8).

The dependence of the absorption spectra of dye **1b** on the concentration of Pb^{2+} ions is described adequately on the basis of the equilibrium

$$L + M \leftarrow LM K_1 = [LM]/([L][M])$$

The corresponding stability constant, log $K_1 = 5.61 \pm 0.02$, was calculated using the Hyperquad program.[11] The complex of **2** with Pb^{2+} is much more stable than that of **1b**. The stability constant of this complex cannot be determined by direct spectrophotometric titration; therefore, it was derived from the data of spectrophotometric titration of complex Pb^{II} [(*E*)-**2**] with benzo-1,10-dithia-18-crown-6 ether (BDT18C6)

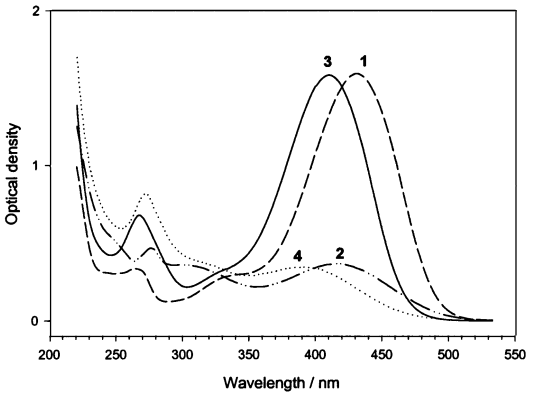

Fig. 7 Absorption spectra of dye **1b** ($C_L = 4 \times 10^{-5}$ M, $l = 10$ mm) in MeCN: *E*-isomer (1), *Z*-isomer (2); in the presence of $Pb(ClO_4)_2$ ($C_M = 7 \times 10^{-5}$ M): *E*-isomer (3), *Z*-isomer (4).

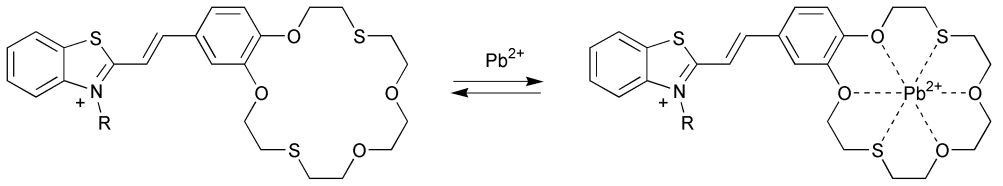

Scheme 6

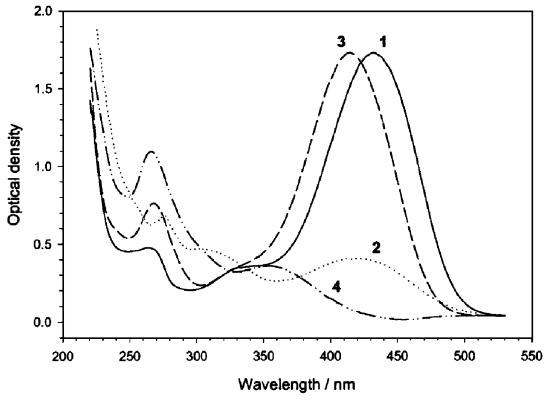

Fig. 8 Absorption spectra of dye **2** ($C_L = 4 \times 10^{-5}$ M, $l = 10$ mm) in MeCN: *E*-isomer (1), *Z*-isomer (2); in the presence of $Pb(ClO_4)_2$ ($C_M = 7 \times 10^{-5}$ M): *E*-isomer (3), *Z*-isomer (4).

as a ligand competitor. The stability constant for the complex of BDT18C6 with Pb^{2+} was previously determined from spectrophotometric data on titration of Pb^{II}[(*E*)-**1b**] with BDT18C6. The complexation model involves two equilibria:

$$L_1 + M \leftarrow L_1M K_1 = [L_1M]/([L_1][M])$$

$$L_2 + M \leftarrow L_2M K_2 = [L_2M]/([L_2][M])$$

where L_1 is **1b**, L_2 is BDT18C6, M is the Pb^{2+} ion, K_1 and K_2 are the the complex stability constants, and K_1 is fixed so that $\log K_1 = 5.61$. The calculated value of $\log K_2$ is 7.26 ± 0.03. The stability constant of complex Pb^{II}[(*E*)-**2**] was calculated from spectrophotometric data on titration of Pb^{II}[(*E*)-**2**] with BDT18C6 for the simplest complexation model, as shown previously for the titration of Pb^{II}[(*E*)-**1b**] with BDT18C6. The stability constant of Pb^{II}[BDT18C6] was fixed such that $\log K_2 = 7.26$, while that for Pb^{II}[(*E*)-**2**] was $\log K_1 = 7.56 \pm 0.05$. The latter value appears to comprise two components, namely, the stability constant for the formation of Pb^{II}[(*E*)-**2**] proper and that for the formation of the $\{Pb^{II}[(E)\text{-}\mathbf{2}]\}_2$ dimer (see below). These constituent stability constants will be measured later and reported elsewhere. The stability constant of complex Pb^{II}[(*Z*)-**2**] was calculated from spectrophotometric data on titration of Pb^{II}[(*Z*)-**2**] with BDT18C6 as a ligand competitor, by analogy with the stability constant determination of complex Pb^{II}[(*E*)-**2**]. Preliminary Pb^{II}[(*Z*)-**2**] was obtained photochemically on irradiation of Pb^{II}[(*E*)-**2**] with a 436 nm light with *E* to *Z* conversion of more than 99%. The stability constant of complex Pb^{II}[(*Z*)-**2**] was $\log K_1 = 8.75 \pm 0.05$.

The conformations of CSDs **1b**, **2**, and their complexes with metal cations can be found from their ^{1}H NMR spectra (Tables 2 and 3). Direct determination of the changes in the proton chemical shifts ($\Delta\delta$) upon complex formation for Pb^{2+} with CSD **2** in MeCN-d_3 is not feasible because the free ligand is not sufficiently soluble in this solvent. Reliable estimates of $\Delta\delta$ were obtained by the use of Mg^{II}[(*E*)-**2**] as the reference ligand. In the complex, the Mg^{2+} cation is linked to the sulfonate group, which increases the solubility of the CSD but does not influence the positions of the aromatic and crown ether methylene protons in the spectrum.[12]

The entire spectrum shifts downfield upon association of metal cations with CSDs **1b** or **2**, the $\Delta\delta$ values being the most pronounced for the methylene hydrogens of the crown ether moiety. The comparison of the $\Delta\delta$ values corresponding to complex formation with Pb^{2+} in MeCN-d_3 for the protons of (*E*)-**1b** and (*E*)-**2** is presented in Tables 2 and 3. The relatively uniform contributions of all oxygen and sulfur atoms of the CSD crown ether moiety to the coordination of Pb^{2+} are reflected in the rather similar $\Delta\delta$ values for all hydrogens of the methylene groups bonded to these heteroatoms. The electron-withdrawing effect of the metal cation in the crown ether cavity is substantially attenuated along the conjugation chain of the chromophore. The most pronounced effect was found for the benzene ring of the benzocrown ether moiety; for benzothiazole, $\Delta\delta$ values are smaller.

Some signals of the Pb^{II}[(*E*)-**2**] complex shift upfield in comparison with the signals of Mg^{II}[(*E*)-**2**], namely, those of H(b), H(5′), and H(6′). This could be due to the fact that Pb^{II}[(*E*)-**2**] exists as the $\{Pb^{II}[(E)\text{-}\mathbf{2}]\}_2$ dimer, in which the mutual influence of the aromatic fragments and the C=C double bonds results in a shielding effect for some protons, as was actually observed for H(b), H(5′), and H(6′). This complex is stable due to the

Table 2 Chemical shifts of the ^{1}H NMR resonances of the aromatic protons of CSDs **1b**, **2** ($C_L = 1 \times 10^{-3}$ M), their complexes with $Pb(ClO_4)_2$ and $Mg(ClO_4)_2$, and cyclobutane **4** ($C_L = 5 \times 10^{-3}$ M) in CD_3CN at 50 °C

		δ								
CSD or complex	CSD:M^{2+} ratio	4	5	6	7	a	b	2′	5′	6′
(*E*)-**1b**		8.03	7.88	7.79	8.20	7.56	8.04	7.50	7.10	7.49
Pb^{II}[(*E*)-**1b**]	1:1	8.07	7.89	7.80	8.23	7.69	8.06	7.65	7.26	7.60
$\Delta\delta = \delta_{Pb^{II}[(E)\text{-}\mathbf{1b}]} - \delta_{(E)\text{-}\mathbf{1b}}$		*0.04*	*0.01*	*0.01*	*0.03*	*0.13*	*0.02*	*0.15*	*0.16*	*0.11*
Mg^{II}[(*E*)-**2**]	1:3	8.10	7.86	7.76	8.20	7.67	8.05	7.59	7.09	7.50
Pb^{II}[(*E*)-**2**]	1:1.1	8.11	7.91	7.83	8.27	7.71	7.89	7.73	7.03	7.24
$\Delta\delta = \delta_{Pb^{II}[(E)\text{-}\mathbf{2}]} - \delta_{Mg^{II}[(E)\text{-}\mathbf{2}]}$		*0.01*	*0.05*	*0.07*	*0.07*	*0.04*	*−0.16*	*0.14*	*−0.06*	*−0.26*
Pb^{II}[(*Z*)-**2**]	1:1.1	8.14	7.95	7.89	8.35	6.70	7.52	7.03	6.91	6.82
$\Delta\delta = \delta_{Pb^{II}[(Z)\text{-}\mathbf{2}]} - \delta_{Pb^{II}[(E)\text{-}\mathbf{2}]}$		*0.03*	*0.04*	*0.06*	*0.08*	*−1.01*	*−0.37*	*−0.70*	*−0.12*	*−0.42*
Pb^{II}_2(**4**)	1:1.1	8.12	7.92	7.86	8.33	4.98	4.44	7.54	7.23	7.54
$\Delta\delta = \delta_{Pb^{II}_2(\mathbf{4})} - \delta_{Pb^{II}[(E)\text{-}\mathbf{2}]}$		*0.01*	*0.01*	*0.03*	*0.06*	*−2.73*	*−3.45*	*−0.19*	*0.20*	*0.30*
Pb^{II}_2(**4**) + 5% D_2O (v/v)	1:1.1	8.11	7.91	7.84	8.31	4.97	4.45	7.44	7.22	7.57

Table 3 Chemical shifts of the ^{1}H NMR resonances of the aliphatic protons of CSDs **1b**, **2** ($C_L = 1 \times 10^{-3}$ M), their complexes with $Pb(ClO_4)_2$ and $Mg(ClO_4)_2$, and cyclobutane **4** ($C_L = 5 \times 10^{-3}$ M) in CD_3CN at 50 °C

		δ										
CSD or complex	CSD:M^{2+} ratio	α	α′	β	β′	γ,γ′	δ,δ′	ε	1″	2″	3″	4″
(*E*)-**1b**		4.33	4.34	3.12	3.16	2.95	3.73	3.61	4.26			
Pb^{II}[(*E*)-**1b**]	1:1	4.64	4.73	3.46	3.51	3.26	4.16	3.97	4.32			
$\Delta\delta = \delta_{Pb^{II}[(E)\text{-}\mathbf{1b}]} - \delta_{(E)\text{-}\mathbf{1b}}$		*0.31*	*0.39*	*0.34*	*0.35*	*0.31*	*0.43*	*0.36*	*0.06*			
Mg^{II}[(*E*)-**2**]	1:3	4.31	4.39	3.14	3.14	2.96	3.73	3.61	4.81	2.21	2.06	2.97
Pb^{II}[(*E*)-**2**]	1:1.1	4.49	4.67	3.38	3.54	3.20	4.09	3.91	4.70	2.13	2.09	3.04
$\Delta\delta = \delta_{Pb^{II}[(E)\text{-}\mathbf{2}]} - \delta_{Mg^{II}[(E)\text{-}\mathbf{2}]}$		*0.18*	*0.28*	*0.24*	*0.40*	*0.24*	*0.36*	*0.30*	*−0.11*	*−0.08*	*0.03*	*0.07*
Pb^{II}[(*Z*)-**2**]	1:1.1	4.48	4.38	3.33	3.20	3.17	4.01	3.85	4.42	1.49	1.34	2.56
$\Delta\delta = \delta_{Pb^{II}[(Z)\text{-}\mathbf{2}]} - \delta_{Pb^{II}[(E)\text{-}\mathbf{2}]}$		*−0.01*	*−0.29*	*−0.05*	*−0.34*	*−0.03*	*−0.08*	*−0.06*	*−0.28*	*−0.64*	*−0.75*	*−0.48*
Pb^{II}_2(**4**)	1:1.1	4.54	4.75	3.39	3.48	3.25	4.07	3.90	4.37	—	—	2.48
$\Delta\delta = \delta_{Pb^{II}_2(\mathbf{4})} - \delta_{Pb^{II}[(E)\text{-}\mathbf{2}]}$		*0.05*	*0.08*	*0.01*	*−0.06*	*0.05*	*−0.02*	*−0.01*	*−0.33*	—	—	*−0.56*
Pb^{II}_2(**4**) + 5% D_2O (v/v)	1:1.1	4.50	4.67	3.36	3.40	3.18	4.00	3.85	4.34	1.61	1.10	2.46

interaction of the *N*-sulfoalkyl substituent of the dye molecule with Pb^{2+} located in the crown ether cavity of the second molecule of **2**. Examination of molecular models of the dimeric complexes based on Pb^{II}[(*E*)-**2**] showed that 'head-to-tail' symmetrical configurations with the crossed arrangment of (*E*)-**2** are most likely for the dimers (dimeric complexes **A**–**D** are presented in Scheme 7). This conclusion is in agreement with theoretical analysis of dimeric Mg^{2+} CSD complexes containing an all-oxygen crown ether moiety.[13]

In dimeric complexes **B** and **C**, the anion substituents are located too far from the crown ether moiety for the formation of a coordination bond between the sulfonate group and the metal cation in the crown ether moiety, so these types of complexes should not be stable. The small upfield shifts observed for H(1″) and H(2″) (Table 3) suggest that dimer **A** is the most probable structure because only in this complex is the sulfoalkyl substituent located in the shielding region of the aromatic residue.

Irradiation of acetonitrile solutions of dyes **1b**, **2**, or their complexes with Pb^{2+} ions by a 365 or 436 nm light induces rapid changes in the absorption spectra, due to reversible *E*–*Z* photoisomerization. The absorption spectra of the *Z*-isomers of dyes **1b**, **2**, and their complexes with Pb^{2+} cations were calculated from the spectra of the corresponding *E*-isomers and the photostationary states obtained during irradiation with 365 and 436 nm light by the Fischer method.[14] The quantum yields in the photoisomerization of Pb^{II}(**2**) are $\varphi_{E-Z} = 0.35$ and $\varphi_{Z-E} = 0.50$.

The absorption spectrum of (*Z*)-**1b**, constructed by application of Fischer's method[14] to the spectrum of a photostation-

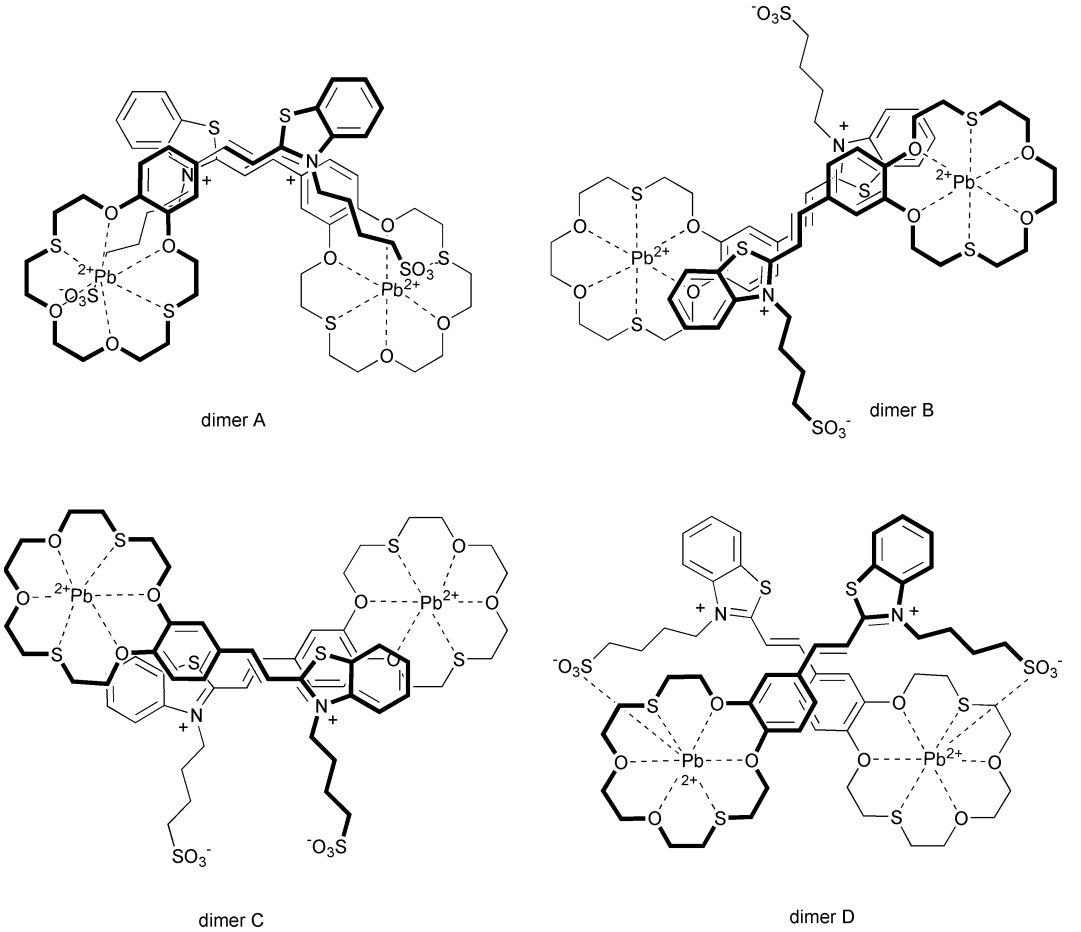

Scheme 7

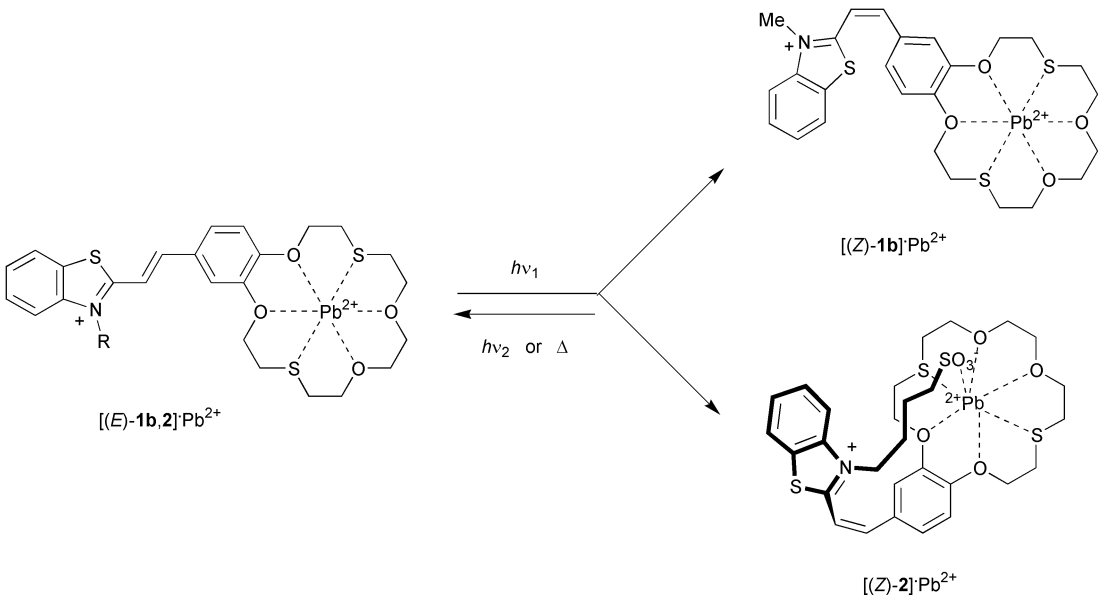

Scheme 8

ary mixture, is shown in Fig. 7, together with the spectrum of (*E*)-**1b** and the spectra of the Pb^{2+} complexes of the two isomers. The spectra of the complexed isomers are remarkably similar to those of the uncomplexed isomers, small (9 and 12 nm, respectively) hypsochromic shifts of the LABs of the *E*- and *Z*-isomers being the major differences induced by complexation. The small shift of the spectrum of Pb^{II}[(*Z*)-**1b**] reveals that complexation does not disturb the interaction of the conjugated moieties in this chromophore and, hence, its nearly planar structure is retained (Scheme 8).

The behaviour of the Pb^{II}[(*E*)-**2**] complex resembles the behaviour of Hg^{II}[(*E*)-**2**], whose *Z*-isomers[9a] have been shown to have an 'anion-capped' structure (Fig. 8). Thus, here we attribute an 'anion-capped' structure to Pb^{II}[(*Z*)-**2**] (Scheme 8). The 63 nm shift of the LAB of Pb^{II}[(*Z*)-**2**] is due to the diminished conjugation between the three moieties comprising the chromophore, consistent with the pronounced departure from planarity which accompanies the formation of 'anion-capped' complexes. Intramolecular coordination in 'anion-capped' Pb^{II}[(*Z*)-**2**] enhances its stability (the K_Z/K_E ratio is 15), causing a sharp deceleration of its dark *Z*–*E* isomerization.

Substantial changes are observed in its ^{1}H NMR spectrum when a solution of Pb^{II}[(*E*)-**2**] is exposed to visible light (Tables 2 and 3). In the novel photoproduct, the spin–spin coupling constants for the olefinic proton signals at 6.70 and 7.52 ppm are 12.2 Hz, which implies the formation of Pb^{II}[(*Z*)-**2**]. In the *Z*-isomer, the signals of the aromatic protons of the benzocrown ether moiety and of the olefinic protons shift upfield, while the benzothiazole proton signals shift downfield relative to those of Pb^{II}[(*E*)-**2**]. The pronounced spectral difference between the two photoisomers is due to the substantial conformational rearrangement induced by the formation of the 'anion-capped' complex (Scheme 8). The formation of this complex enforces a twisted conformation on the chromophore, resulting in a distortion of the conjugated system and concentration of the positive charge in the benzothiazole fragment of the molecule. The greatest changes were found for the resonances of the H(a) and H(2′) protons, which is apparently due to the fact that the protons fall into the areas of shielding of the benzothiazole fragment and the double C=C bond.

Due to the possibility of spontaneous assembly giving rise to a dimeric complex with a determined architecture, CSDs can be used as synthons for stereospecific photochemical synthesis of cyclobutanes containing thiacrown ether fragments. We found that irradiation of the complexed forms of (*E*)-**2** with 436 nm light leads to consumption of the dye, which occurs in parallel with the formation of the *Z*-isomer. Virtually complete consumption of **2** in $Pb(ClO_4)_2$-containing solutions was reached over reasonable time periods upon photolysis with 365 nm light. Fig. 9 shows the absorption spectrum of the photolyzate resulting from [2 + 2]-photocycloaddition (PCA). In the absence of a metal cation, CSD **2** does not undergo PCA under the above-mentioned conditions. For CSD **1b**, the PCA reaction occurs neither in the presence nor in the absence of metal cations.

Detailed analysis of the structure of the photolysis product was done for Pb^{II}[(*E*)-**2**] using COSY and NOESY 2D techniques and by comparison with available ^{1}H NMR spectral data for the cyclobutanes of the benzothiazole series.[8d,15] The ^{1}H NMR spectrum of the photoproduct **4** in MeCN-d_3 (Table 2) exhibits two triplets at 4.44 and 4.98 ppm due to the protons of the cyclobutane ring. The absence of olefinic protons with typical coupling constants $^3J_{trans} = 15.6$ or $^3J_{cis} = 12.2$ Hz provides additional evidence for the disappearance of **2**. The phototransformation yields only one isomer, **4**, which is responsible for an A_2B_2-type spectrum with $^3J_{trans} = 9.6$ Hz. The quantity, position, multiplicity, and spin–spin coupling constants of the cyclobutane ring protons in **4**, constructed according to the *anti*-'head-to-tail' pattern, are similar to those

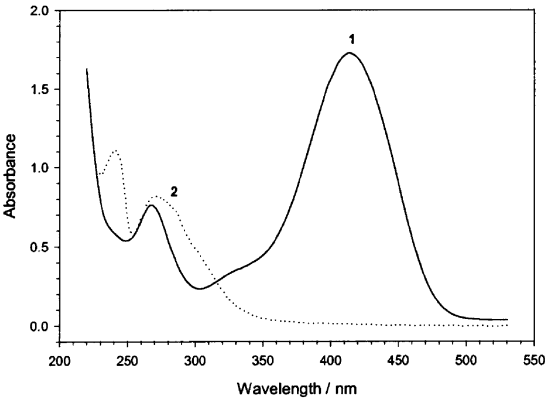

Fig. 9 Absorption spectra in the presence of $Pb(ClO_4)_2$ ($C_M = 7 \times 10^{-5}$ M) in MeCN: (1) *E*-isomer of dye **2** ($C_L = 4 \times 10^{-5}$ M, $l = 10$ mm); (2) cyclobutane **4** ($C_L = 2 \times 10^{-5}$ M, $l = 10$ mm).

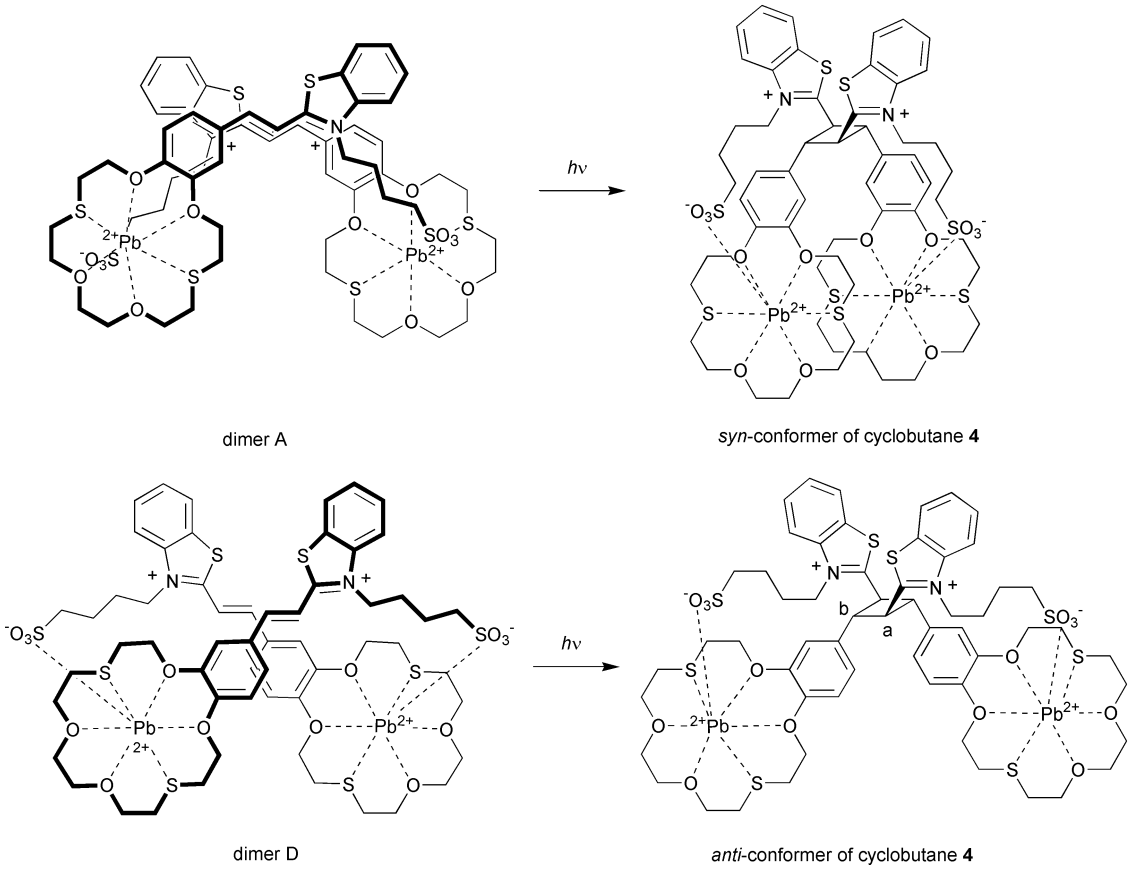

Scheme 9

obtained for cyclobutanes of the benzothiazole series.[8d,15] The cyclobutane with the all-*trans* arrangement of substituents could have been formed from dimeric complexes **A** or **D**. The cycloadduct resulting from dimer **A** should be produced as the *syn*-conformer, while photocycloaddition with the participation of dimer **D** should lead to the *anti*-conformer (Scheme 9). The NMR analysis reveals that the chemical shifts of the H(2′) (Table 2) and H(1″)–H(4″) (Table 3) peaks are located at higher field than those for Pb^{II}[(*E*)-**2**]. According to the space-filling models for the *syn*- and *anti*-conformers of **4**, only in the *anti*-conformer does the proton H(2′) fall in the shielding region of the benzothiazolium fragment and are the H(1″)–H(4″) spacer protons located closely above the benzene ring fragment. This suggests that the cyclobutane **4** is produced from dimer **D**. The facts that dimer **A** contains non-parallel C=C double bonds and dimer **D** is a minor component account for the low quantum yield of photocycloadditon ($\Phi_{PCA} = 10^{-3}$).

Thus, the spontaneous formation of dimeric complexes comprising two dye molecules and two metal cations with a fixed mutual arrangement of the double bonds provides a pre-organization of the reactants favourable for regio- and stereoselective [2 + 2]-photocycloaddition.

Monolayer investigation

The amphiphilic CSD **3** forms relatively stable monolayers over distilled water and various aqueous salt subphases. The collapse pressure of the dye monolayer is about 25.5 mN m^{-1} for distilled water or in the range 25.3–26.4 mN m^{-1} in the presence of Na^+, K^+, Mg^{2+}, or Ca^{2+} ions in the aqueous subphase (Fig. 10). These values, which represent the stability of the monolayer of CSD **3**, are significantly lower than those for monolayers of similar CSDs containing a benzodithia-15-crown-5 ether fragment.[5b] This can be explained by the higher solubility of **3** in the aqueous subphase, especially at high surface pressures, due to the larger size of the crown ether ring. The collapse pressure of the monolayer of **3** increases to 49.0 mN m^{-1} in the presence of Ag^+ ions in the aqueous subphase (Fig. 10, curve 3), the first indication of strong complexation of CSD **3** with Ag^+, which significantly stabilizes the dye monolayers compared to those over water or solutions of alkali metal cations.

The area per molecule of CSD **3** at monolayer collapse is smallest on water (0.39 nm^2) and increases slightly in the presence of K^+, Na^+, Mg^{2+}, or Ca^{2+} ions in the aqueous subphase (0.41, 0.44, 0.43, and 0.44 nm^2, respectively). In spite of the small collapse area for the monolayers of CSD **3** with Ag^+ (0.39 nm^2), related to the very high collapse pressure

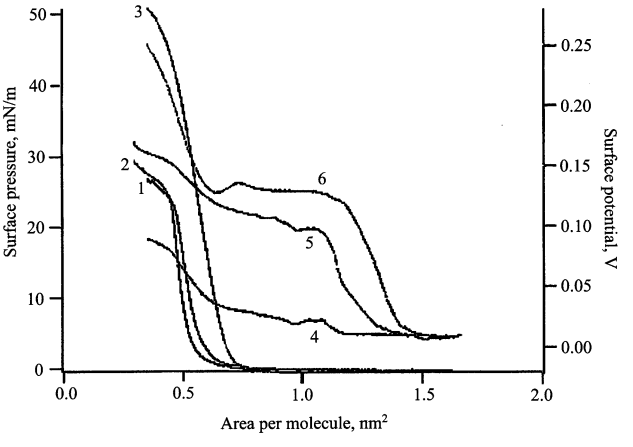

Fig. 10 Surface pressure–molecular area and surface potential–molecular area isotherms for CSD **3** monolayers on water (1,4) and 1 mM solutions of NaCl (2,5) and $AgClO_4$ (3,6) at 20 °C.

(49 mN m^{-1}), the area at 5 mN m^{-1} is significantly greater (0.67 nm^2) than that in the case of CSD **3** monolayers over other salt solutions (0.56, 0.55, 0.54, and 0.54 nm^2 areas at 5.0 mN m^{-1} on water, K^+, Na^+, Mg^{2+}, and Ca^{2+} ions, respectively). It is important to emphasize that CSD **3** only shows a liquid-condensed state in the whole range of monolayer areas and pressures (no transition is observed, Fig. 10). All the data obtained to date can be interpreted by assuming the existence of two different types of dye–cation complexes in the monolayers: (i) weak complexes in the case of alkali and alkaline earth metal cations (probably, due to the specific interaction of the cation with the O atoms of the macrocycle) and (ii) strong complexes in the case of Ag^+ ions (probably, due to the specific interaction of the cation with the S atoms in the dithia polyether ring of the dye molecule).

This explanation is also applicable to the differences in the surface potential values (ΔV) for the dye on various aqueous salt subphases (Fig. 10). First, upon compression, the absolute surface potentials of the CSD **3** monolayers on water increase gradually, while those on all the salt solutions studied increase sharply. Second, whereas the ΔV values in the case of K^+ and Na^+ (145 and 159 mV, respectively) are significantly higher than those for water (only about 75 mV), in the case of Ag^+ (227 mV), this value is even higher. Third, there is a slight decrease in ΔV values (after passing through a maximum) upon further monolayer compression in the case of K^+ and Na^+. This could be due to a transition from 1:1 to 1:2 cation–dye complexes because of preferential interaction of alkali metal cations with 8 O atoms (1:2 complex) instead of 4 O atoms (1:1 complex). Fourth, in the case of Ag^+, there is an expanded plateau for ΔV values of about 125–130 mV in a wide range of monolayer areas (from 1.10 to 0.70 nm^2) followed by a gradual increase to about 100 mV upon increasing the surface pressure (from very low values to the collapse pressure) upon the monolayer compression in the whole range of molecular areas.

The reflection spectra (plotted as the difference, DR, of the reflectivity of the monolayer-covered subphase and that of the clean subphase[16]) of CSD **3** monolayers on distilled water and various salt solutions exhibit a strong band in the range 400–500 nm (with a small shoulder at 490–500 nm for some salts) and a less intense band at 330–340 nm. The reflection maximum for the CSD **3** monolayers over distilled water is about 428 nm at 5 mN m^{-1}. There is a small increase in DR from 0.246 to 0.279 for dye monolayers on water (without any shift of the maximum position) following an increase in the surface pressure from 1 to 25 mN m^{-1}. Qualitatively the same spectra are observed for the dye monolayers in the presence of K^+ (the maximum is at about 426–428 nm) or Na^+ ions in the aqueous subphase (the maximum is at about 428–430 nm) over the whole range of surface pressures. An increase in the reflection intensity at the maxima following an increase in the surface pressure from 1 to 25 mN m^{-1} was observed in the presence of K^+ (from 0.272 to 0.365) or Na^+ (from 0.311 to 0.342) with respect to water. We attribute this to a combination of the following factors: (i) the increasing surface density of the chromophores and (ii) the change in their orientation upon monolayer compression. In contrast, there is an opposite shift of the reflection band maximum for the dye monolayers in the presence of Ag^+ ions (from 428 to 422 nm upon increasing the surface pressure from 1 to 30 mN m^{-1}) in the aqueous subphase, but the DR increases only slightly (from 0.259 to 0.278) as the surface pressure increases over the same range. This can be interpreted as being due to strong complexation of the dye by heavy metal cations present in the aqueous subphase and dimerization of the dye molecules in the monolayer due to complexation with the Ag^+ cations. Additional evidence for molecular dimerization is the pronounced shoulder at 490–500 nm, observed only for dye monolayers in the presence of Ag^+, but not with alkali metal cations. Thus, it is possible to distinguish two types of dye monolayer structures, depending on the presence of alkali or heavy metal cations in the aqueous subphase.

Conclusions

We report in this paper different types of assemblies of CSD molecules in crystals, solutions, and films in the presence of metal cations. In the crystalline state, the anion affects the supramolecular architecture of the CSD. This conclusion is general for all types of crown ether dyes and it allows the supramolecular architecture of crown ether styryl dye cations to be controlled by changing the counter ion.

In solution, cationic CSDs can form complexes with Pb^{2+} whose spectral characteristics and photochemical behaviour are close to those of the initial dye. Alternatively, CSDs with the betaine structure spontaneously form dimeric complexes in the presence of Pb^{2+}, comprising two dye molecules and two metal cations with a fixed mutual arrangement of the double bonds. The photochemical behaviour of this supramolecular complex differs substantially from that in the initial ligand molecule. Irradiation of the complex dimers induces regio- and stereoselective [2 + 2]-cycloaddition. The other photoreaction carried out for CSDs is the reversible *E*–*Z* isomerization, resulting in the 'anion-capped' *Z*-isomer.

The amphiphilic CSD **3** forms relatively stable monolayers on alkaline earth metal salt and silver salt aqueous subphases. The results obtained indicate that the characteristics of the monolayers depend on the type of salt present in the subphase. This effect implies that the metal cation influences the molecule arrangement in monolayers. These results could be useful for the preparation of monolayers with desirable characteristics.

Experimental

X-Ray diffraction analysis

The molecular geometry of **1a** has been briefly described previously.[8a] The corresponding structural parameters are available from the Cambridge Crystallographic Database (REFCODE KEDNAI). The crystals of **1a** and **1b** were grown from acetonitrile solutions. The crystallographic data and the parameters of structure solution and refinement are given in the ESI. Both structures were solved by direct methods and non-hydrogen atoms refined anisotropically. All hydrogen atom positions were calculated geometrically and included in the refinement using the riding model. In **1a**, one of the crown ether atoms, S(1), is disordered over two positions S(1A) and S(1B), with equal occupancies. In structure **1b**, the S(2), C(8), and C(9) atoms show rather high mean-square atomic displacements. This is apparently due to the disordering of the C(8)S(2)C(9) fragment over several positions. The location and magnitude of the residual electron density peaks in the vicinity of this crown ether fragment also correspond to another, minor, component of disordering.

The XCAD4[17] sofware was used for data reduction in the case of **1a** and the Siemens SAINT[18] software, in the case of **1b**. The SHELXS-86[19] and SHELXL-93[20] software were used for structure solution and least-squares refinement over F^2, respectively.

CCDC reference number 166224. See http://www.rsc.org/suppdata/nj/b1/b110630a/ for crystallographic data in CIF or other electronic format.

Synthesis of the complexes of (*E*)-1b and (*E*)-2 with $Pb(ClO_4)_2$

$Pb(ClO_4)_2$ (0.00055 mmol) and (*E*)-**1b** or (*E*)-**2** (0.00055 mmol) were dissolved in 0.55 mL of CD_3CN under red light. The resulting complexes Pb^{II}[(*E*)-**1b**] and Pb^{II}[(*E*)-**2**] were used for

the NMR investigations and for the preparation of Pb^{II}[(*Z*)-**1b**] and Pb^{II}[(*Z*)-**2**].

Synthesis of the complexes of (*Z*)-1b and (*Z*)-2 with $Pb(ClO_4)_2$

A solution of Pb^{II}[(*E*)-**1b**] or Pb^{II}[(*E*)-**2**] in CD_3CN (0.5 mL, $C_L = 5 \times 10^{-4}$ M) was irradiated at 436 nm. This gave isomeric mixtures containing more then 98% Pb^{II}[(*Z*)-**1b**] or Pb^{II}[(*Z*)-**2**], which were used for the NMR investigations.

Synthesis of the cyclobutane derivative 4

A solution of dye **2** (0.01 mmol) and $Pb(ClO_4)_2$ (0.0125 mmol) in dry acetonitrile (5 mL) was irradiated with light from a DRK-120 mercury lamp at 365 nm for several hours. When the dye was wholly consumed (monitoring by UV-Vis spectroscopy), the acetonitrile was evaporated *in vacuo*. A partially uncomplexed form of **4** was obtained upon the addition of D_2O (5%, v/v) to the $Pb(ClO_4)_2$-containing solution of **4** in CD_3CN.

UV-Vis spectra

A Specord-M40 spectrophotometer was used. The preparation of solutions and all experiments were carried out under red light. Photochemical experiments were carried out by exposing solutions of CSDs and their metal complexes to filtered 365 (1.4×10^{15} intensity) or 436 nm (9.8×10^{14} cm^{-2} s^{-1} intensity) light from a DRK-120 mercury lamp. The individual mercury lines of the spectrum of this lamp (313, 365, 405 and 436 nm) were isolated by the use of glass filters.

The quantum yields of $E \rightarrow Z$ and $Z \rightarrow E$ photoisomerizations (φ_{t-c}, φ_{c-t}) and PCA (φ_{PCA}) for the complex of **2** with $Pb(ClO_4)_2$ were determined upon irradiation of solutions at 365 nm.

^{1}H NMR study

The ^{1}H NMR spectra were recorded at 323 K on a Bruker DRX-500 spectrometer operating at 500.13 MHz for protons. The chemical shifts were measured with an accuracy of 0.01 ppm, and the spin–spin coupling constants were determined with an accuracy of 0.1 Hz. A sample of the cyclobutane derivative obtained from $\{Pb^{II}[(E)\text{-}2]\}_2$ was dissolved in CD_3CN and D_2O was then added. The COSY and NOESY 2D spectra were recorded using the standard Bruker pulse sequences (cosy45, cosygs, noesytp, roesyprtp) and processed using the Bruker XWINNMR program. The mixing time for the NOESY spectra was 700 ms, the delay between the experiments was 2 s, and the number of scans per experiment was 32. A total of 512 f1 points and 2048 f2 points were accumulated. The signals in the ^{1}H NMR spectra of Mg^{II}[(*E*)-**2**], Pb^{II}[(*E*)-**2**], and cyclobutane derivative **4** were assigned based on the NOEs obtained during the NOESY experiments.

Monolayer study

Monolayers of surface-active monomers were prepared and studied on a Lauda FW-2 film balance. The samples of monomers (10 mL from 10 mM solutions) were spread onto a 1.0 mM phosphate buffer subphase at pH 7.0 and 20 °C, between the moving and measuring barriers. The monolayers were compressed by moving the barrier with a constant speed of about 1 cm^2 s^{-1}; the surface pressure–molecular area and surface potential–molecular area isotherms for the monolayer were recorded.

The reflection spectra of the crown ether dye monolayers on water or various aqueous salt solutions at chosen surface pressures were recorded directly at the gas–liquid interface, as described previously.[16]

Acknowledgements

Financial support from the Royal Society, the Deutsche Forschungsgemeinschaft, the INTAS (grant 2001-0267), the Russian Foundation for Basic Research (projects no. 01-03-32474, 00-03-32159, 00-03-32898 and 00-03-33238), and the Ministry for Science and Technologies of Russia is gratefully acknowledged.

References

1 (*a*) V. Balzani and F. Scandola, *Supramolecular Photochemistry*, Ellis Horwood, Chichester, 1990; (*b*) J.-M. Lehn, *Supramolecular Chemistry*, VCH, Weinheim, Germany, 1995; (*c*) F. Vögtle, *Supramolecular Chemistry*, Wiley, Chichester, 1993; (*d*) S. P. Gromov and M. V. Alfimov, *Russ. Chem. Bull.*, 1997, **46**, 611.

2 (*a*) J. S. Connolly and J. R. Balton, in *Photoinduced Electron Transfer*, ed. A. M. Fox and M. Chanon, Elsevier, Amsterdam/New York, 1988, part D; (*b*) H. Kurreck and M. Huber, *Angew. Chem., Int. Ed. Engl.*, 1995, **34**, 849.

3 (*a*) J.-P. Sauvage, *Acc. Chem. Res.*, 1998, **31**, 611; (*b*) V. Balzani, S. Campagna, G. Denti, A. Juris, Sc. Serroni and M. Venturi, *Acc. Chem. Res.*, 1998, **31**, 26.

4 (*a*) *The Crystal as a Supramolecular Entity*, ed. G. R. Desiraju, Wiley, Chichester, 1995; (*b*) R. Robson, B. F. Abrahams, S. R. Batten, R. W. Gable, B. F. Hoskins and J. Liu, *Supramolecular Architecture*, ACS, Washington, DC, 1992, ch. 19; (*c*) M. V. Alfimov, A. V. Churakov, Y. V. Fedorov, O. A. Fedorova, S. P. Gromov, R. E. Hester, J. A. K. Howard, L. G. Kuz'mina, I. K. Lednev and J. N. Moore, *J. Chem. Soc., Perkin Trans. 2*, 1997, 2249

5 (*a*) I. K. Lednev and M. C. Petty, *Adv. Mater.*, 1996, **8**, 615; (*b*) S. Yu. Zaitsev, E. A. Baryshnikova, T. I. Sergeeva, S. P. Gromov, O. A. Fedorova, O. V. Yescheulova, M. V. Alfimov, S. Hacke, W. Zeiss and D. Möbius, *Colloids Surf.*, 2000, **171**, 283; (*c*) S. Yu. Zaitsev, T. I. Sergeeva, E. A. Baryshnikova, W. Zeiss, D. Möbius, O. V. Yescheulova, S. P. Gromov, O. A. Fedorova and M. V. Alfimov, *Mater. Sci. Eng., C*, 1999, 469.

6 (*a*) *Comprehensive Supramolecular Chemistry*, ed. J.-M. Lehn, Pergamon Press, New York, 1996; (*b*) B. L. Feringa, W. F. Jager and B. de Lange, *Tetrahedron*, 1993, **49**, 8267; (*c*) *Applied Fluorescence in Chemistry, Biology, and Medicine*, ed. W. Rettig, B. Strehmel, S. Schrader and H. Seifert, Springer-Verlag, Berlin, 1999.

7 (*a*) H. Bouas-Laurent, A. Castellan and J.-P. Desvergne, *Pure Appl. Chem.*, 1980, **52**, 2633; (*b*) H. Bouas-Laurent, A. Castellan, M. Daney, J.-P. Desvergne, G. Guinand, P. Marsua and M.-H. Riffaund, *J. Am. Chem. Soc*, 1986, **108**, 315.

8 (*a*) S. P. Gromov, O. A. Fedorova and M. V. Alfimov, *Mol. Cryst. Liq. Cryst.*, 1994, **246**, 183; (*b*) S. I. Druzhinin, M. V. Rusalov, B. M. Uzhinov, S. P. Gromov, S. A. Sergeev and M. V. Alfimov, *J. Fluor.*, 1999, **9**, 33; (*c*) E. N. Ushakov, S. P. Gromov, A. V. Buevich, I. I. Baskin, O. A. Fedorova, A. I. Vedernikov, M. V. Alfimov, B. Eliasson and U. Edlund, *J. Chem. Soc., Perkin Trans. 2*, 1999, 601; (*d*) S. P. Gromov, O. A. Fedorova, E. N. Ushakov, A. V. Buevich, I. I. Baskin, Y. V. Pershina, B. Eliasson, U. Edlund and M. V. Alfimov, *J. Chem. Soc., Perkin Trans. 2*, 1999, 1323.

9 (*a*) M. V. Alfimov, S. P. Gromov, Yu. V. Fedorov, O. A. Fedorova, A. I. Vedernikov, A. V. Churakov, L. G. Kuz'mina, J. A. K. Howard, S. Bossmann, A. Braun, M. Woerner, D. F. Sears and J. Saltiel, *J. Am. Chem. Soc.*, 1999, **121**, 4992; (*b*) M. V. Alfimov, Yu. V. Fedorov, O. A. Fedorova, S. P. Gromov, R. E. Hester, I. K. Lednev, J. N. Moore, V. P. Oleshko and A. I. Vedernikov, *J. Chem. Soc., Perkin Trans. 2*, 1996, 1441; (*c*) M. V. Alfimov, Y. V. Fedorov, O. A. Fedorova, S. P. Gromov, R. E. Hester, I. K. Lednev, J. N. Moore, V. P. Oleshko and A. I. Vedernikov, *Spectrochim. Acta, Part A*, 1997, **53**, 1853.

10 (*a*) I. I. Baskin, A. A. Bagatur'yants, S. P. Gromov and M. V. Alfimov, *Dokl. Akad. Nauk*, 1994, **335**, 313 (in Russian); (*b*) A. Ya. Freidzon, I. I. Baskin, A. A. Bagatur'yants, S. P. Gromov and M. V. Alfimov, *Russ. Chem. Bull.*, 1998, **47**, 2117.

11 P. Gans, A. Sabatini and A. Vacca, *Talanta*, 1996, **43**, 1739.

12 M. V. Alfimov, A. I. Vedernikov, S. P. Gromov, Yu. V. Fedorov and O. A. Fedorova, *Russ. Chem. Bull.*, 1997, **46**, 2099.

13 M. V. Alfimov, S. P. Gromov, O. B. Stanislavsky, E. N. Ushakov and O. A. Fedorova, *Russ. Chem. Bull.*, 1993, **42**, 1385.

14 E. Fischer, *J. Phys. Chem.*, 1967, **71**, 3704.

15 (*a*) S. P. Gromov, E. N. Ushakov, O. A. Fedorova, A. V. Buevich and M. V. Alfimov, *Russ. Chem. Bull.*, 1996, **45**, 722; (*b*) S. P. Gromov, O. A. Fedorova, E. N. Ushakov, I. I. Baskin, A. V. Lindeman, E. V. Malysheva, T. A. Balashova, A. S. Arsenjev

and M. V. Alfimov, *Russ. Chem. Bull.*, 1998, **47**, 97; (*c*) S. P. Gromov, O. A. Fedorova, E. N. Ushakov, A. V. Buevich and M. V. Alfimov, *Russ. Chem. Bull.*, 1995, **44**, 2131.
16 M. Orrit, D. Möbius, U. Lehmann and H. Meyer, *J. Chem. Phys.*, 1986, **85**, 4966.
17 K. Harms, XCAD4, Program for the Lp-Correction of Nonius CAD4 Data, University of Marburg, Germany, 1997.
18 SAINT, Program for Area Detector Absorption Correction, Siemens Analytical X-Ray Instruments Inc., Madison, WI, USA, 1995.
19 G. M. Sheldrick, *Acta Crystallogr., Sect. A*, 1990, **46**, 467.
20 G. M. Sheldrick, SHELXL-93, Program for the Refinement of Crystal Structures, University of Göttingen, Germany, 1993.